Valentin Zuchuat
Research scientist
val.zuchuat@csiro.au
CSIRO
26 Dick Perry Ave, Kensington WA 6151

csiro.au | ABN 41 687 119 230

Perth, February 2025

Review of manuscript "AstroComb(v.1.0): Non-linear, Multi-channel, Probabilistic Cyclostratigraphic Analysis" by Fernandes et al.

Dear editor, dear authors,

I would like to thank you for giving me the opportunity to review the manuscript titled "AstroComb(v.1.0): Non-linear, Multi-channel, Probabilistic Cyclostratigraphic Analysis" by Fernandes et al. The manuscript introduces AstroComb, a probabilistic, multi-channel cyclostratigraphic algorithm that estimates locally varying (possibly discontinuous) sedimentation rates by fitting Milankovitch targets in the frequency domain. The method is demonstrated on high-resolution CS-XRF records from the late Cambrian Alum Shale (Fågeltofta-2 core) and on synthetic data with very high red noise. Both code and data are openly available, which I command the authors for!

The new workflow presents some strong innovative features, notably including the omission of smoothing, that allows for abrupt sedimentation-rate fluctuations to be considered, accompanied by an uncertainty estimate. As a sedimentologist and basin stratigrapher, this attribute is extremely powerful.

The manuscript requires some updates, though, in order to be accepted for publication in EGUSphere.

My first comment is not directed at the authors, but at the journal editors. Please invite the journal to update their templates with new sans-serif fonts. Indeed, with-serif fonts (e.g. times new roman), which are the ones used in EGUSphere templates right now, are much more difficult to read than sand-serif fonts (e.g. arial), especially for people with vision impairment or reading difficulties. I would also suggest to add a "Use of AI-tool" disclaimer at the end of the manuscript.

The manuscript requires major revisions to be accepted for publication. I would suggest the authors to address all the following comments, as well as the detailed comments on the commented-pdf attached to this letter.

1. Autogenic processes and signal shredding

I recommend the authors to acknowledge autogenic processes and signal shredding explicitly (rivers/deltas, compensational stacking; see commented pdf for references examples). It is also necessary to clarify how AstroComb distinguishes or remains agnostic to these signals vs. orbital forcing. The authors could consider adding a short paragraph in Introduction and returning to it in Discussion. An easy way to start with this is to take some of the text from the "limitations" chapter.

I also suggest the authors to avoid the term "geological noise" for non-Milankovitch periods. The preserved signal might not be "noise", but rather the true expression of the mix of autogenic processes, Milankovitch cycles, and other non-linear effects such as bundling of several cycles. It is also important to justify why AstroComb does not include such periods (lines 311-314).

2. Scope

Other software are briefly mentioned (l. 31-33). Also this paper remains quite diplomatic about how much better AstoComb is in comparison to these other software, the reader of this manuscript could do with a figure that displays how the different software deal with the same input dataset.

The manuscript also only use single elements or several single elements together. A lot of published research (see references in the attached commented pdf) study change in Earth System conditions through the use of elemental-concentration ratios as well as enrichment factors. It could be useful to show how AstoComb responds to elemental-concentration ratios and enrichment factors.

Finally, it would be beneficial for the manuscript to compare the results from the conformable Alum Shale Formation to other sedimentary-cores XRF scans much more impacted by event beds, hiatus, or vacuity. This would allow the authors to highlight how AstroComb deals with these extreme changes in sediment supply. If this is not possible, please add a short demonstration in addition to your synthetic example, or at least discuss applicability in greater detail. Doing so would allow you to confirm, precise, or disagree with published sedimentation rates of other sedimentary units.

3. Methods chapter

I would like the authors to add in the method chapter a paragraph on their XRF data collection workflow: add model, tube type, kV/mA, measurement time, temperature, calibration/normalisation, etc. The authors could also cite the paper that generated these data in the first place.

4. Results and interpretations

I would suggest to move beyond "visual examples" and describe the results in great details. For instance, the figures displaying the age-model: how does this relate to the sedimentation rates? Where do abrupt changes occur (e.g. line 326); how large are these abrupt changes; over what thickness/time do they occur; what geological interpretations are plausible? Why are some intervals "less Milankovitch" than others in your "information content" curve, tie all of this to core observations and geochemical data.

I would also recommend the authors to have all the figures 3-4-5-6-7 plotted as a one-pager figure together. This will allow for a much easier comparison between the single-element run and the multiple single-element run. Additionally, to tie this comment back to the previous one, please quantify the difference between the to runs, rather than having these results as visual examples. And add the elemental curves used for each runs to these figures.

Doing so will allow the authors to expand the discussion to the interpretation of the succession they have studied in great detail.

5. Figures and presentation

I would invite the authors to highlight and indicate more features on their figures: for example, where are the sedimentation rates changing "abruptly", whare are the "spurious features" that "could be interpreted as true sedimentation rate" (l. 289-290), etc.

I would suggest adding element-curves to Fig. 3-6-10 next to the information content curve, which x-axis need to have a unit or an explanation as to why it doesn't have one. Add proposed sedimentation rate curves on all probability plots, just like you have done on Fig. 10. The authors are also invited to quantify the difference between the two runs.

The authors are also invited to combine Fig. 8-9-10 in a one-page figure as well. Please rotate the Fig. 9 to have the depth as a vertical axis, just like all the other figures. Please quantify the impact of "However, the test also shows how artifacts are introduced by the noise, the variability of the true model, and the non-linearity of the problem" (caption of Fig. 10), which are concept that should be discussed in greater detail by the authors, especially with regards to the results of the studied core Fågeltofta-2.

Please check the journal reference formatting, as there seem to be many unnecessary parentheses when multiple references are cited in the text.

Please chose and stick to "ky", "kyr", or "kyrs" for consistency. Similarly, always call the core Fågeltofta-2, rather than a mix of Fågeltofta-2 or Fågeltofta (e.g. caption of Fig. 2, or l. 304, 326)

Please use the official chronostratigraphic series name Furongian as opposed to late/upper Cambrian.

If the authors have any questions on my comments, please feel free to contact me directly.

Dr Valentin Zuchuat

AstroComb(v.1.0): Non-linear, Multi-channel, Probabilistic Cyclostratigraphic Analysis

Iris Fernandes[*1], Klaus Mosegaard[1], Aske L. Sørensen[2], Mohammad Youssof[1], Nicolas Thibault[2], and Tais W. Dahl[2]

[1]Niels Bohr Institute, University of Copenhagen, Denmark
[2]Department of Geosciences and Natural Resource Management, University of Copenhagen, Denmark

Abstract

We present a new algorithm for constructing floating astronomical timescales with explicit uncertainty estimates from sedimentary sequences. The method integrates probabilistic spectral analysis with inverse geochronological modeling, applied to ultra-high-resolution, multiproxy datasets such as core scanning X-Ray Fluorescence (XRF) elemental records. Our framework does not smooth data or impose layer-to-layer dependency, allowing sedimentation rates to vary abruptly at short stratigraphic length scales. By detecting and statistically constraining Milankovitch cycles preserved in stratigraphic signals, the algorithm seeks a floating age-depth model that can be anchored to astronomical tie points, where available. The resulting timescales enable precise, uncertainty-bounded timing of biostratigraphic zones, geochemical events, and depositional cycles. This approach advances astrochronology by combining cycle detection with formal stratigraphic modelling, while preserving fine-scale depositional variability, offering a reproducible and statistically rigorous framework for dating deep-time records.

1 Introduction

Stratigraphic records from sedimentary basins are powerful archives of past environmental variability, recording both long-term geological trends and short-term changes in Earth's climate system. Identifying and decoding these Milankovitch cycles provides an essential tool for reconstructing past timescales — a methodology known as astrochronology.

Traditional astrochronologic approaches typically rely on matching repetitive spectral features in stratigraphic depth-series data to a target set of orbital frequencies, either through spectral filtering (Hays et al. (1976); Weedon (2003); Meyers et al. (2008, 2001)), or tuning

---
*Corresponding author: iris@nbi.ku.dk

against numerical astronomical solutions (`TimeOpt`: Meyers (2015), `TimeOptMCMC`: Meyers and Malinverno (2018); `AstroGeoFit`: Hoang et al. (2025)) or evolutionary spectral correlation (`eCOCO`: Li et al. (2018), `eTimeOpt`: Meyers (2019)).

Despite sedimentation is a punctuated process (Kemp and Sexton (2014)) over shorter timescales, these cyclostratigraphic methods often assume continuous, smoothly varying sedimentation rates or enforce strict stationarity in cycle expression over longer time scales; e.g. precession period. As a result, current age-depth models likely oversimplify the stratigraphic record, particularly in cases where sedimentation is punctuated by hiatuses, erosion, rapid deposition events, authigenic sediment, diagenetic ~~chemical~~ alteration or lithologic transitions. In reality, sediment accumulation in marine basins is controlled by a complex interplay of sediment supply, accommodation ~~space,~~ bottom water conditions, and diagenesis — all of which can introduce non-uniformity in the sedimentation rate at fine scales.

The continuity-assumption becomes problematic especially over shorter stratigraphic thickness representing shorter time scales. For example, the approximately 500 million year-old Cambrian Alum Shale Formation of Scandinavia has been slowly-deposited, and the shortest Milankovitch periods (19 kyrs) are covered by only 2–12 cm of stratigraphy (Sørensen et al. (2020); Zhao et al. (2022)). Here, we advocate that spectral matching to target periodicities must be done probabilistically, and astrochronological models must accommodate uncertainty in the depositional response to the forcing signal. ~~Fortunately,~~ these shales consists of finely laminated mud (grain size $\approx 2\,\mu m$) and high-resolution elemental datasets can be obtained at sub-millimeter resolution using Core Scanning X-Ray Fluorescence (CS-XRF) spectroscopy providing opportunities and challenges for refining astrochronological timescales including rigorous error propagation that requires more sophisticated analytical tools.

In response to these challenges, we present a probabilistic method to infer instantaneous sedimentation rates directly from multi-channel geochemical time series data (e.g. elemental abundances or ratios) by fitting Milankovitch cycles in a locally adaptive manner. Rather than assuming a constant or globally smoothed rate model, our approach treats sedimentation as a piecewise continuous process, allowing for abrupt or non-linear changes across the stratigraphic column. The core innovation is to invert a forward model of spectral signal generation — simulating how Milankovitch frequencies are expressed across stratigraphic depth under varying sedimentation rates — to obtain the probability distribution of the sedimentation rate at each depth, conditioned on observed multi-channel data and a target astronomical signal.

This framework is implemented in a newly developed algorithm, `AstroComb`, which builds upon and extends the concepts behind earlier astrochronological tools, such as `TimeOptMCMC` (Meyers and Malinverno (2018) and `eCOCO` Li et al. (2018)), while incorporating uncertainty quantification adapted to high-speed computation on large, multi-channel data sets. `AstroComb` applies a windowed, sliding inversion across the stratigraphy, yielding a depth-resolved series of sedimentation rates and posterior uncertainties. `AstroComb` allows discontinuities in sedimentation rate where supported by the data — for example, in the presence of condensed layers, stratigraphic breaks, or sharp facies transitions — which may be essential for reconstructing realistic depositional histories. Furthermore, `AstroComb` provides a measure of the information content of the data at all depths, indicating the uncertainty/reliability of the sedimentation rate estimates. Importantly, `AstroComb` calculates the full probability

76 distribution of sedimentation rates based on multi-channel input data, which is essential
77 input for sub-precession cycle refinement of age-depth relationships using geochemically-
78 informed sedimentation rates as exercised with `ProBE4T` (Fernandes et al. (2026)).

79 Here, we apply `AstroComb` to the Fågeltofta-2 core through the ~~later Cambrian~~ Alum
80 Shale Formation. The core comprises a thick, continuous succession of laminated, organic-
81 rich, black mudrocks with high pyrite content and strong enrichments in redox sensitive
82 elements (Dahl et al. (2019)). The Alum shale was deposited extremely slowly ($\sim$ 1–6 mm/ky,
83 Nielsen et al. (2018)) on the Baltoscandian passive margin. Using high-resolution XRF data
84 from over 90,000 measurements across 18 m of stratigraphy at 0.2 mm intervals, previous
85 cyclostratigraphic analyses have confirmed such slow sedimentation rates (Sørensen et al.
86 (2020); Zhao et al. (2022)), which we here show are also consistent with `AstroComb` results
87 presented here. Further, the `AstroComb` results reveal abrupt variation in sedimentation
88 rates, potentially identifying intervals of slow background accumulation interspersed with
89 short-duration accumulation events. Potentially, chemical oscillations allow for improved
90 dating of stratigraphic intervals, ~~duration of event,~~ and lithologic transitions within the core
91 — with implications for rates of paleoenvironmental change and refinement of the geological
92 time-scale.

93 `AstroComb` is designed to leverage high-resolution multi-element core data for astrochronol-
94 ogy in a quantitative probabilistic manner. The algorithm aligns a range of astronomical
95 periods with recurring signals in the stratigraphy, and extends the capabilities of previous
96 toolboxes by incorporating multichannel geochemical data and uncertainty quantification
97 through inverse modeling at each analysis step. Each channel represent elemental abun-
98 dance (in peak area or concentrations), best fit mineral abundance (in weight percent) or
99 ratios between XRF peaks areas (e.g. Al/RhCoh, normalized peak area signals).

100 The overarching goal is to detect Milankovitch signals and construct floating astronomical
101 timescales, while explicitly accounting for uncertainties. The approach is built on four main
102 components, which constitute the workflow of `AstroComb`:

103 • A probabilistic inversion framework to recover, not only the best-fit sedimentation rate
104 at any given stratigraphic point in an elemental time series, but also uncertainties and
105 a measure of information content.

106 • A generalizable methodology that can be applied to any cyclic geochemical or pale-
107 oenvironmental signal,

108 • A demonstration of how variable sedimentation rates manifest in the spectral expres-
109 sion of Milankovitch cycles

110 • An application to a $\sim$500 Ma Cambrian core verifies the preservation of astronomical
111 signals and evaluate sedimentation rates and their probability distributions (uncer-
112 tainty) from the information content.

113 By integrating multi-element signal processing, spectral modeling, and inversion theory, our
114 approach extends the methodological framework of astrochronology into previously unex-
115 plored domains. It enables the simultaneous analysis of multiple signals and accommodates
116 probabilistic age–depth models that can be non-smooth, and discontinuous—reflecting the
117 inherent complexity of real-world sedimentary systems.

2 Theory and Methods

2.1 Overview

The goal of this study is to reconstruct a *locally varying sedimentation rate profile* from multiple geochemical depth series, under the assumption that certain stratigraphic signals (e.g., elemental variability) reflect astronomical forcing. We achieve this by inverting a forward model of signal distortion under varying sedimentation, using a formulation rooted in probabilistic inversion.

This method builds upon the principles of astrochronology—particularly the spectral identification of Milankovitch-band periodicities in sedimentary records—but extends them to allow for *instantaneous, non-stationary sedimentation rates*. `AstroComb` performs a sliding-window probabilistic fit of observed geochemical spectra to a predefined target astronomical spectrum, yielding a sedimentation rate that optimally "stretches" or "compresses" the time axis at each position to recover astronomical frequencies. The fit is performed in frequency domain, which allows multi-channel (e.g. multiple elements) that will not be obscured if displaced by a phase-lag.

We begin by formalizing the relationship between sedimentation rate and spectral distortion, then describe the inversion procedure and implementation of `AstroComb`. Finally – as an example – we discuss its application to the Alum Shale data and compare to previous results (Sørensen et al. (2020)).

2.2 Forward Model of Spectral Distortion

Let $d(z)$ be a geochemical depth series (e.g., Al concentrations), where z is stratigraphic depth. If sediment accumulated at a locally constant rate $r(z) = \frac{dz}{dt}$, then in the time domain, the corresponding series is $d(t)$. However, in practice we only observe the signal in the depth domain.

Let k be a frequency in the depth domain (wave number in cycles per mm) and f its time-domain counterpart (cycles per kyr). The transformation between the two is:

$$k = \frac{f}{r} \tag{1}$$

Thus, a fixed astronomical frequency f will appear in the stratigraphic record as a peak at k, depending on the local sedimentation rate. Variations in $r(z)$ distort the signal, shifting, splitting, or smearing spectral peaks. Our objective is to recover $r(z)$ such that the observed power spectrum matches that predicted from astronomical forcing (see Figure 1).

2.3 Target Astronomical Spectrum

Because no closed form orbital solution exists beyond about 50 Ma (Laskar et al. (2011, 2004)), we adopt theoretical periods constructed from studies of deep-time orbital mechanics (Farhat et al. (2022); Waltham (2015)). For the later Cambrian $\sim$ 497 Ma, the target includes:

- Long eccentricity: 405 kyr

154 • Short eccentricity: 99 ky

155 • Obliquity: 32.4 kyr

156 • Precession: 19.5 kyr

157 We encode these as 4 sinusoids with known periods. We do not define their expected
158 spectral power ratios based on orbital modulation transfer, since the Earth's climate and
159 environmental response to the Milankovitch forcing modifies these ratios in an unknown
160 way.

2.4 Computing the Likelihood of a Sedimentation Rate

162 For a given depth interval (window) centered at z_0, we obtain power spectra $\mathbf{D}_{obs}$ of multiple,
163 observed signals ($\mathbf{D}_{obs}$ is a matrix of spectra with a spectrum of one channel in each column).
164 For each trial sedimentation rate r, we convert the target time-domain frequencies f to
165 expected depth-domain frequencies (wave numbers) $k = f/r$ and compute *synthetic spectra*

$$\mathbf{G}(r, \mathbf{a}) = \sum_{m=1}^{M} a_m \mathbf{w} \left(\frac{f_m}{r} \right) \tag{2}$$

166 where $\mathbf{G}(r, \mathbf{a})$ is a matrix of computed data spectra (a copy of the spectrum in each column),
167 f_m is the m'th Milankovitch frequency (assumed known), and $\mathbf{w}(\frac{f_m}{r})$ is the shape of a spectral
168 line, centered at $\frac{f_m}{r}$. The shape $\mathbf{w}$ can be computed as the discrete Fourier transform of a
169 discretized delta function with the same length as the window.

170 From the synthetic spectra $\mathbf{G}(r, \mathbf{a})$ and the matrix of observation spectra $\mathbf{D}_{obs}$ we can
171 now calculate the likelihood as the probability of data, given the sedimentation rate r and
172 the spectral peak amplitudes $\mathbf{a}$:

$$L(r, \mathbf{a}) = P\left(\mathbf{D}_{obs} | (r, \mathbf{a}) \right). \tag{3}$$

173 Our computation of the likelihood is done as follows:

174 1. As prior information about the data uncertainties, we mimic the 'manual' process of
175   spectral line identification by defining a probability that there is a potential Milankovic
176   peak at a given wavenumber k in the spectrum. Between user-defined lower and upper
177   bounds a (the lower limit for being identified as a "peak") and b (the value above which
178   we are sure that we have found a potential peak), the probability increases from a user
179   defined, small positive number p_a at the lower limit to $p_b = 1 - p_a$ at the upper limit.
180   Typical values are $a = \langle F \rangle + \sigma_F$ and $b = \langle F \rangle + 3\sigma_F$, where $\langle F \rangle$ is a local mean of the
181   spectrum around the considered wavenumber k, and σ_F is the local standard deviation
182   of the spectrum. A typical value of the threshold probability p_a is 0.01. The probability
183   is chosen as a smooth, monotonically increasing sigmoid function $p(x)$ satisfying

$$p(a) = p_a, \qquad p_b(b) = 1 - p_a, \tag{4}$$

184 with the constraints

$$b > a, \qquad 0 < p_a < 0.5. \tag{5}$$

We adopt the logistic sigmoid form

$$p(x) = \frac{1}{1 + \exp\big(-k(x - x_0)\big)} \tag{6}$$

with

$$x_0 = \frac{a + b}{2}. \tag{7}$$

2. For each layer (which is $\Delta z = 0.2$ mm thick in the Fågeltofta-2 core example), we evaluate the likelihood in a grid of sedimentation rates r with typical grid spacing $\Delta r = 0.02$ mm/ky. Each possible choice corresponds to given locations of the Milankovic cycles in the spectrum, and for each location at k_i with spectral amplitude a_i, we evaluate the probability $p(k_i, a_i)$. Finally, the likelihood of the considered sedimentation rate $\mathbf{r}$ is computed as the product

$$L(\mathbf{r}) = \prod_{i=1}^{I_M} p(k_i, a_i), \tag{8}$$

where I_M is the number of Milankovic cycles considered. When several records of, e.g., basic elements concentrations are used in the calculation, the combined likelihood for all records is computed as the product of the individual likelihoods.

2.5 The Posterior Probabilities of Sedimentation Rates

If prior information about $(r, \mathbf{a})$ is encoded by a probability density $\rho(r, \mathbf{a})$ we can - in a Bayesian formulation - express the complete, probabilistic solution as a *posterior* probability density

$$p(r, \mathbf{a}) = C \cdot L(r, \mathbf{a}) \, \rho(r, \mathbf{a}). \tag{9}$$

where C is a proportionality constant. In the example below, where data from Fågeltofta-2 is analyzed, the prior assigns constant values to all sedimentation rates within user-defined boundaries of 1.0 mm/ky $< r <$ 10.0 mm/ky.

From the marginal sedimentation rate distribution

$$p(r) = \int p(r, \mathbf{a}) \; da \tag{10}$$

at each stratigraphic position, we can now compute a floating geological time, t, and its uncertainties as a function of depth, z. If the absolute time, t_0, is known at a given depth z_0, and the sedimentation rate in layer n is r_n, the time at $z_0 + N\Delta z$ is

$$t(z_0 + N\Delta z) = t_0 + \Delta z \sum_{n=1}^{N} \frac{1}{r_n} \; . \tag{11}$$

From the posterior probability densities of the sedimentation rates r_n, and hence $\Delta z / r_n$, we can now calculate the uncertainties of the times. From the variances of the distributions of $\Delta z / r_n$ for all layers n, we can obtain the variance of $t(z_0 + N\Delta z)$ by a simple summation:

$$Var(t(z_0 + N\Delta z)) = \sum_{n=1}^{N} Var\left(\frac{\Delta z}{r_n}\right) \; . \tag{12}$$

210 Working with variances, instead of the full probability distributions for the inverse sedimen-
211 tation rates, saves computer storage and time when processing large data sets. Furthermore,
212 due to the central limit theorem, the distribution of the sum of random time increments
213 will converge to a Gaussian distribution when the number of layers increases, making the
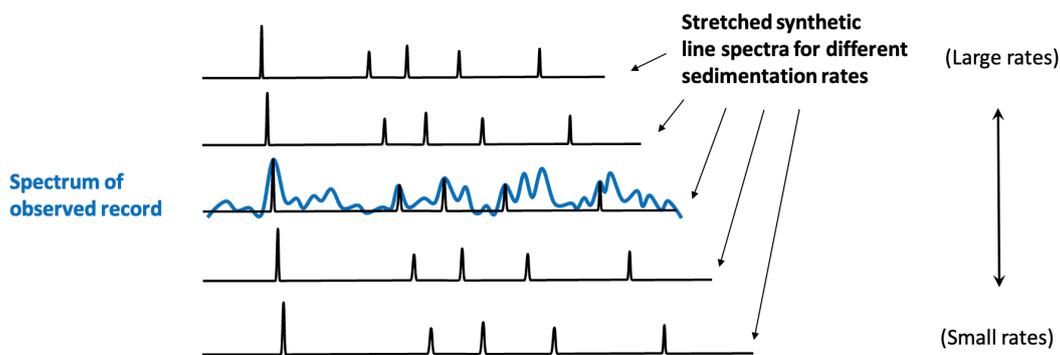214 variance an adequate description of the uncertainty.

Figure 1: Schematic overview of the likelihood calculation for fitting Milankovitch cycles in ele-
mental profiles. The spectrum of the observed geochemical signal (e.g., Al content) is compared
against a theoretical line spectrum, composed of known astronomical frequencies, and stretched ac-
cording to the sedimentation rate. The likelihood of each assumed sedimentation rate is computed
from the probabilities that amplitudes at line locations are significant peaks. This process yields
probability distributions of sedimentation rates as a function of depth, and allows an age–depth
model consistent with Milankovitch forcing to be computed.

2.6 The AstroComb Algorithm

216 AstroComb implements the above approach through the following steps:

217 1. **Preprocessing**: Detrend and normalise the depth series, optionally re-sample or
218   smooth.

219 2. **Sliding Window**: For each depth window (e.g., 2–4 m interval), compute the local
220   power spectrum.

221 3. **Spectral Inversion**: Fit the observed spectrum to the target astronomical model and
222   estimate the posterior probability distribution of the sedimentation rate.

223 4. **Output**: Store the sedimentation rate $r(z)$ and its posterior probability distribution
224   for the window.

225 Every step in our calculation is accompanied by an uncertainty estimate. For each position
226 of the sliding data window, the total noise on the signal (measurement noise on the data
227 from the XRF scanner, and "geological noise" defined as signal that is not measurement
228 noise or Milankovic signal) is automatically estimated by the algorithm (see the likelihood
229 calculation above).

3   Results

To illustrate the application of the multichannel, probabilistic Milankovitch period detector, AstroComb, we analysed high-resolution XRF data from a ∼20-meter long interval of the Fågeltofta-2 drill core through the Alum Shale Formation in southern Sweden. Given that the XRF measurements were collected with a sampling resolution of 0.0002 meters and captured the concentrations of at least 22 elements, incl. Al_2O_3, SiO_2, S, K_2O, CaO, TiO_2, V, MnO, Fe_2O_3, Ni, Cu, Zn, Ge, As, Rb, Sr, Y, Zr, Mo, Ba, Hf, and U, this extensive elemental dataset formed the basis for the spectral analysis. Figure 2 shows a subset (the top 40 mm) of the data from ∼19 m of core, yielding ∼90,000 measurements.

We simultaneously searched for 4 canonical Milankovitch periods applicable to the late Cambrian area at 494 Ma based on Waltham (2015), grouped as follows:

- **Precession** (in ky): 19.5

- **Obliquity** (in ky): 32.4

- **Eccentricity** (in ky): 405, 99
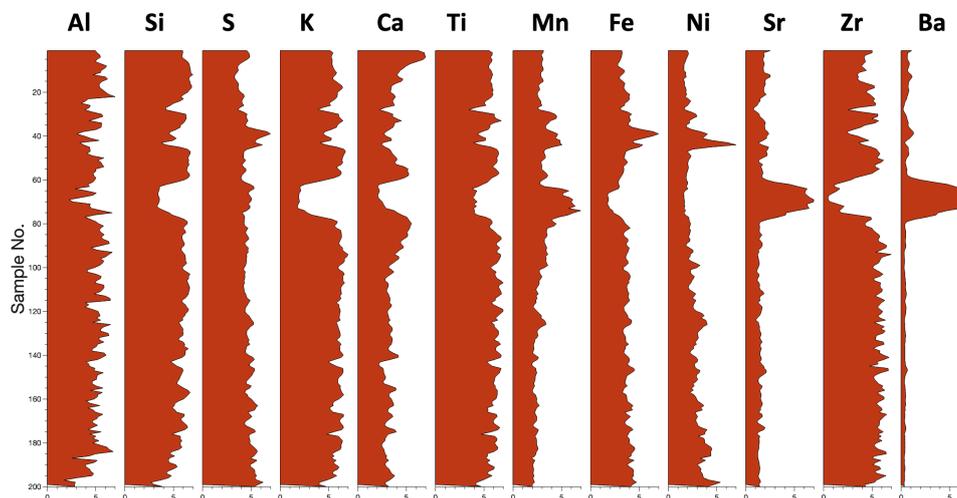
Figure 2: A selection of concentration profiles of the Fågeltofta Alum Shale core, measured via XRF core scanning at 0.2 mm resolution. The dataset spans approximately 19 meters of stratigraphy and comprises ∼ 90,000 individual measurements. Several profiles show well-developed quasi-periodic oscillations, which serve as the primary proxy for detecting orbitally forced sedimentary cycles in the subsequent astrochronological analysis.

We selected Al as the primary input because of its robustness as a proxy for detrital input and its strong spectral structure in preliminary analysis (Sørensen et al. (2020); Zhao et al. (2022)). The depth series was detrended with a linear function. AstroComb was run using a window length of 3.3 m, stepped every 0.2 mm.
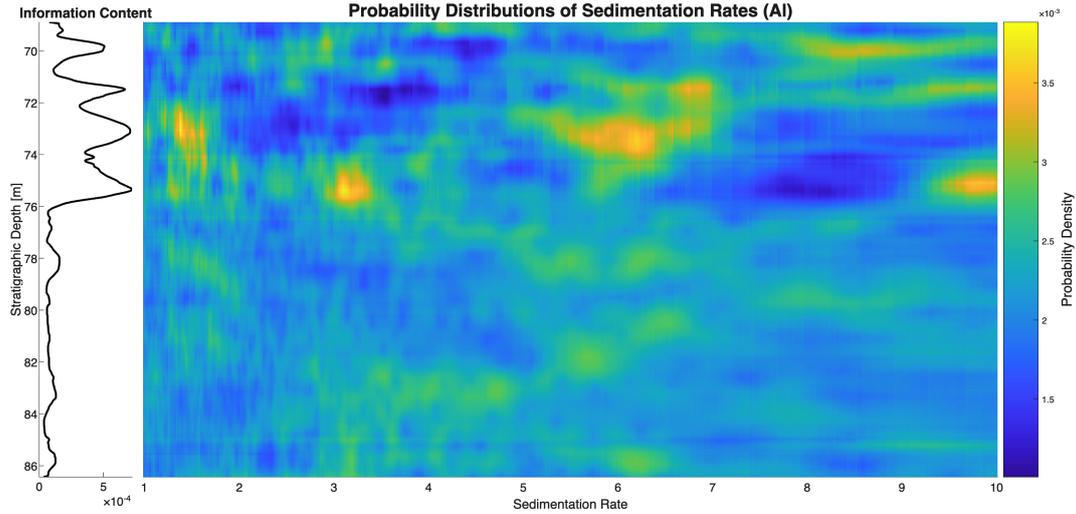
Figure 3: Sedimentation rate probability distribution for the Fågeltofta-2 core. The information content about Milankovic cycles contained in the XRF data is shown (green curve) as quantified by the Kullback-Leibler measure.

The bulk sedimentation rate was *a priori* found within a range of realistic sedimentation rates from 1.0 to 10.0 mm/ky. As output, we show the a posteriori probability distribution of the sedimentation rates versus stratigraphic depth (figure 3), and selected spectral fits for each 2 m in the core (figure 4). Also, we introduce the Kullback-Leibler information measure at each depth z showing how much Milankovic information is present in the data as a function of depth. This is obtained from:

$$\mathcal{I} = \int_R P_z(r) \ln \left(\frac{P_z(r)}{U(r)} \right) dr \tag{13}$$

where $P_z(r)$ is the calculated probability distribution of r at depth z, R is the range of sedimentation rates, and $U(r)$ is a uniform (non-informative) distribution. Figure 3 shows that Milankovic cycles information is present in the core, and that the sedimentation rates vary also within information-dense intervals.

From the estimated sedimentation rates, a Milankovitch timescale and its uncertainty was derived (Figure 5), using the age of 496.595 Ma, consistent with Sørensen et al. (2020), at a stratigraphic depth of 86.005 m as a reference. This timescale enables the estimation of relative geological ages across the core, and allows depth-indexed chemical data to be analysed in the temporal domain, significantly enhancing our ability to interpret environmental transitions over geological timescales.

To demonstrate ASTROCOMB's capability of multi-channel analysis of several basic elements records to obtain improved resolution of the Milankovic cycles, we simultaneously ran the algorithm on the S, Al and Mn records. The result, which is given in figure 6, shows that

9

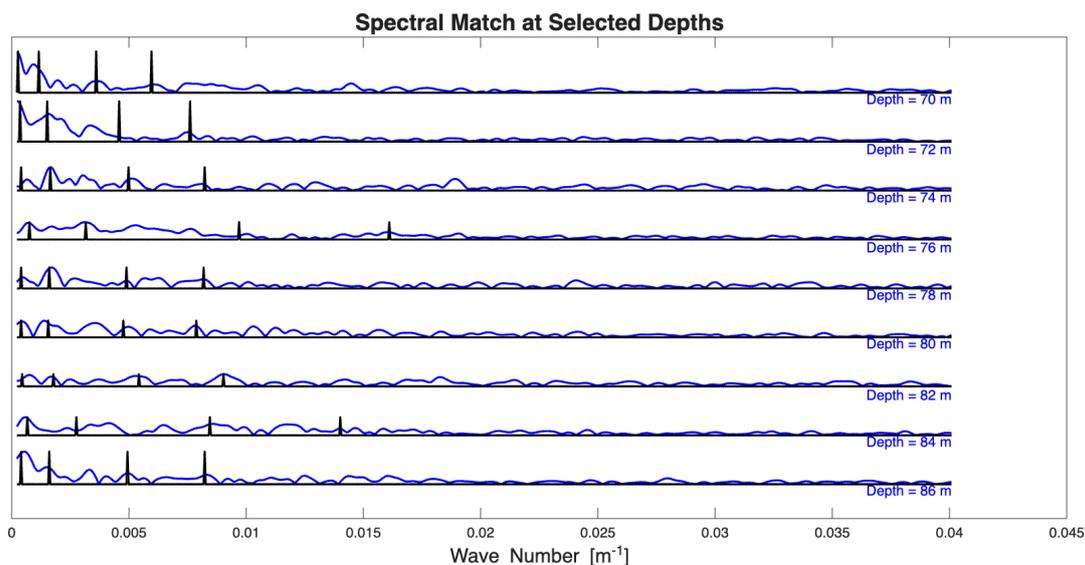Figure 4: Spectral match at selected stratigraphic depths in the Fågeltofta-2 core. For every 2 m, the spectral lines corresponding to the best Milankovic match are plotted together with spectra of data observed in windows centered at the depth.
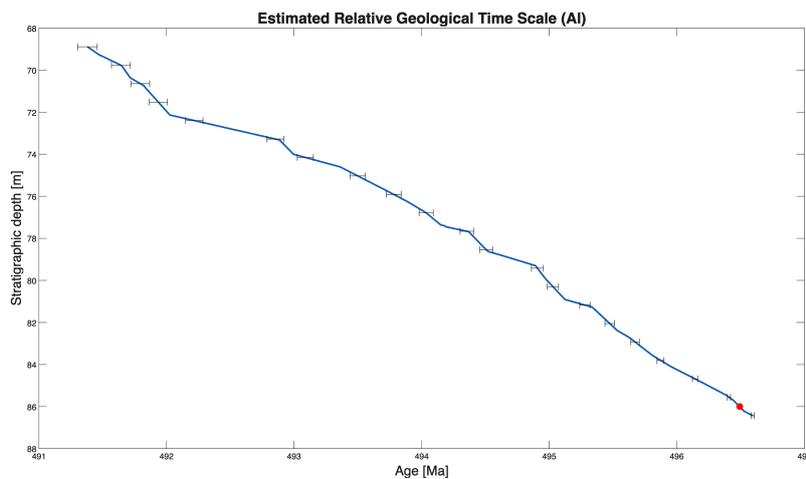

Figure 5: Estimated geological timescale and its uncertainty (standard deviations), based on probabilistic estimation of instantaneous sedimentation rates from the Al record in the Fågeltofta-2 core. The timescale is anchored at 86.005 m, corresponding to 496,595 ky (Sørensen et al. (2020)). This is marked on the graph.
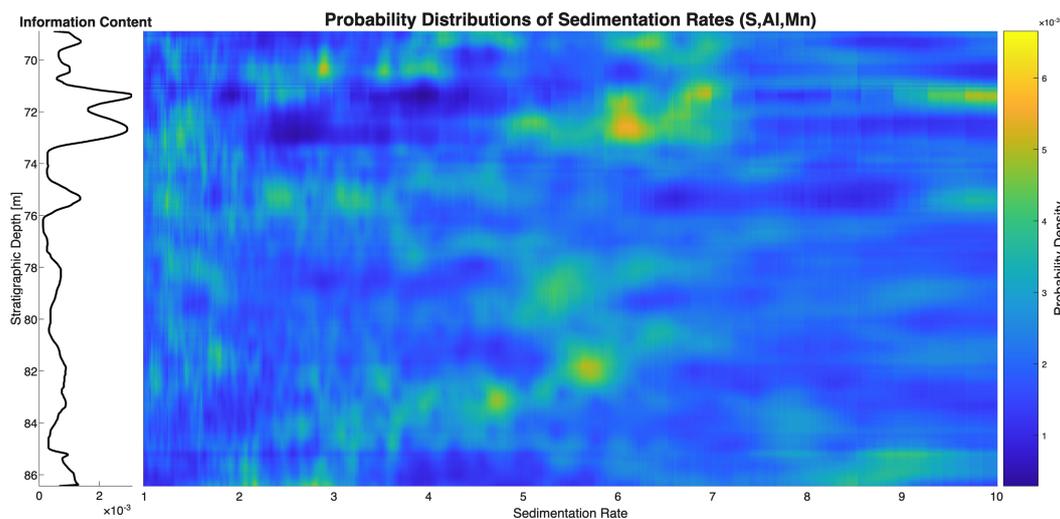
.

Figure 6: Probabilistic analysis of sedimentation rates in the Fågeltofta-2 core, based on simultaneous processing of S, Al, and Mn. Comparing to figure 3 it is clear that this multi-channel analysis has provided a higher resolution with more distinct peaks in the probability densities.

the resolution has improved, compared to the single-channel result in figure 3. High probabilies have increased, and low probabilities have decreased. The overall picture is generally the same, but several secondary peaks, indicating possible alternative solutions, are reduced or have disappeared. The corresponding relative time scale is shown in figure 7. The overall picture is similar to figure 5, but there is more detail, and the total time span is somewhat increased.

The results support the use of high-resolution XRF data coupled with probabilistic spectral inversion as a powerful tool for extracting geochronological information from ancient sedimentary archives.

4 Discussion

Extensive tests were carried out to study the accuracy and stability of the algorithm. A severe test with artificial data with 200% noise, showing significant sedimentation rate discontinuities, was carried out. The synthetic sedimentation rate model, seen in figure 8, is characterized by layers with realistic sedimentation rates, and separated by significant discontinuities. From this model, the synthetic data were calculated (see figure 10). The 200% noise was red noise with a $1/f^2$ power spectral density, simulating a background spectrum of geological signal that cannot be explained as astronomical forcing. Figure 10 shows the posterior probability densities of sedimentation rates for all depths, computed by `AstroComb` using the synthetic data. The true result (the synthetic model) is overlain to show the fidelity
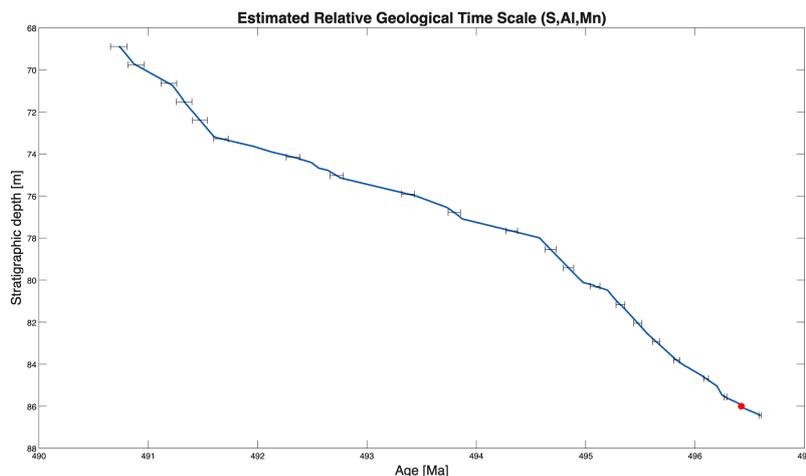
Figure 7: Relative timescale computed from the multi-channel data with records of S, Al and Mn.

of the reconstruction. Considering the very high noise level, the reconstruction of the true
sedimentation rates is excellent. However, the test also illustrates how artifacts (possible,
incorrect sedimentation rates) are introduced by the noise, the variability of the true model,
and the non-linearity of the problem. Some of these spurious features could be interpreted as
true sedimentation rates. This is a challenge, but, on the other hand, all true sedimentation
rates are found by the algorithm, and the large discontinuities beteen layers of constant rates
are quite well reconstructed, despite the high noise level.

This study demonstrates that the `AstroComb` method extends the spectral misfit min-
imization strategy in a probabilistic framework, handling uncertainty propagation and pa-
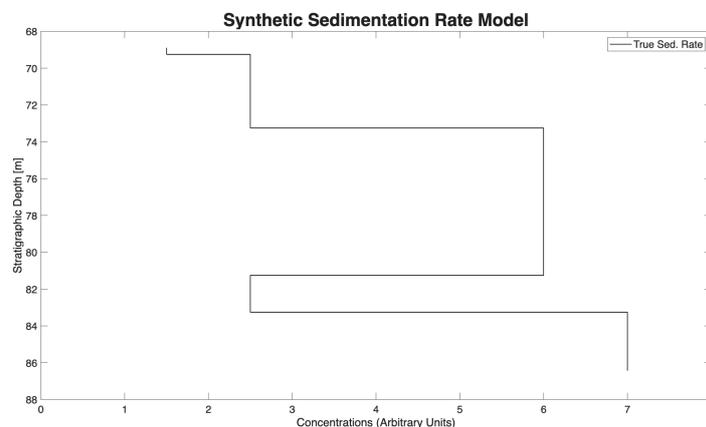rameter tuning with statistical rigor.

Figure 8: Synthetic sedimentation rate model used in the testing of the algorithm. The model has
layers with realistic sedimentation rates, and the layers are separated by significant discontinuities.
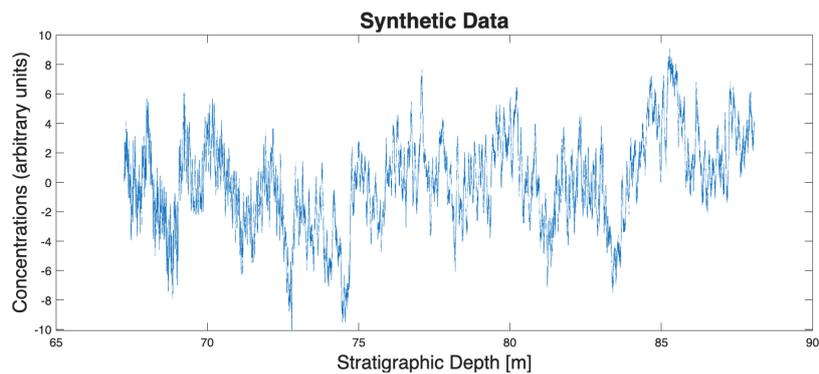
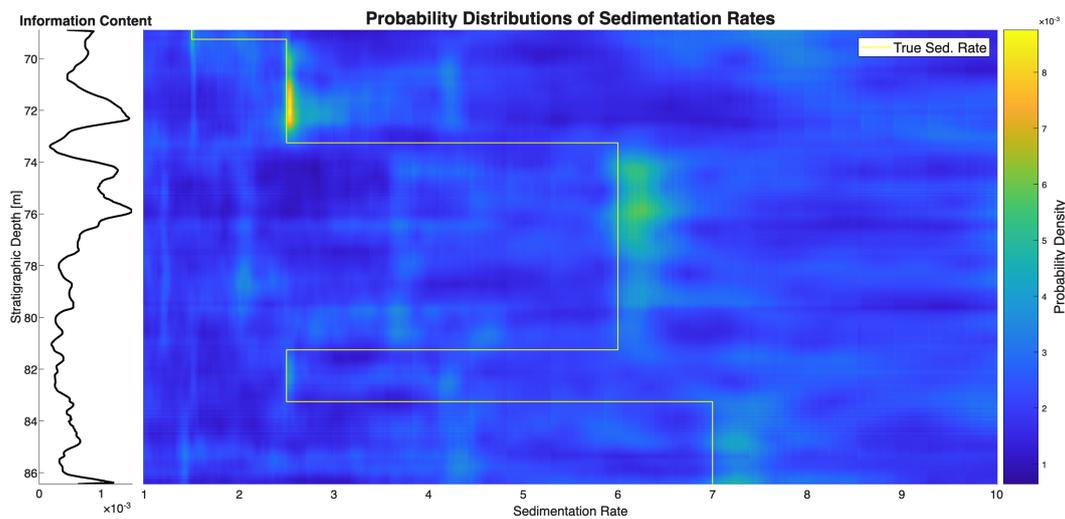Figure 9: Synthetic data with 200% red noise used to test of the algorithm.

Figure 10: Probability densities of sedimentation rates, computed from the synthetic data with 200% red noise. The synthetic model is overlain to show the fidelity of the reconstruction. In view the very high noise level, the reconstruction of the true sedimentation rates is very good. However, the test also shows how artifacts are introduced by the noise, the variability of the true model, and the non-linearity of the problem.

4.1 Limitations

Nonetheless, some limitations must be acknowledged. The assumed orbital target periods are model-based and cannot be empirically verified for the Cambrian. While the tuning strategy relies on the 405 kyr eccentricity cycle as a stable chronometer, potential shifts in Earth's rotational parameters due to e.g. tidal dissipation effects could introduce biases.

Our algorithm is based on the assumption that prior information about the spectral peak identification process can be provided, and that it adequately describes the way Milankovic periods are identified by human analysts. According to our synthetic tests, and the good consistency of our Fågeltofta results with results from previous studies, it works well, but it is advisable to carefully check results obtained in new cases, particularly to what extent they are compatible with other, independent knowledge about the geological scenario considered.

There are also some fundamental assumptions behind Milankovic analysis that apply to any method. Milankovic cycles are (quasi-)periodic, but not sinusoidal. This means that a hypothetical, noise-free Milankovic spectrum will, in general, contain spectral components outside the main Milankovic frequencies. These components are generally disregarded in Milankovic analysis programs, including `AstroComb`. More seriously, the Earth's sedimentary system is highly nonlinear and is therefore expected to produce additional periods that are sums and differences of the main Milankovic cycles. The amplitudes of such periods could be significant, but they are ignored by our algorithm. An additional problem with the nonlinearity of the sedimentary system is that, even if we know the amplitudes of the input Milankovic signal, the output amplitudes observed in boreholes are entirely unknown. This was the background for the the way that we implemented our spectral fit algorithm.

Last, but not least, it is important to remember that Milankovic cycle identification is a *difficult* problem. The signal-to-noise ratio is generally very low, and the problem is often similar to finding a needle in a hay stack. Such problems are prone to detrimental human biases, but `AstroComb` is designed with the aim of quantifying the analysis, and casting the problem as a probabilistic inference problem, so as to avoid such biases. It generally provides several plausible solutions for the sedimentation rates at given depths, allowing the user to choose, based on geological/stratigraphic knowledge.

4.2 Broader Implications

The `AstroComb` algorithm has discovered abrupt changes in sedimentation rate in the Fågeltofta core, making predictions to guide sedimentologist in reconstructing pulses of sedimentation from geological archives. As sedimentation rate is a fundamental parameter characterizing a sedimentary environment and a factor that serves as a first order control on organic matter preservation, `AstroComb` may help engaging sedimentologists with a new relative chronometer. Also, we envision to use it in combination with geochemical information about sedimentation rate changes.

5 Conclusion

Our algorithm contributes methodologically to the field of deep-time astrochronology by offering a multi-channel, probabilistic method for estimation of astronomically constrained

timescales. At the same time we offer critical quality control of the data, allowing the user to evaluate how much Milankovic information can actually be detected in the basic elements records. The framework established here provides a robust platform for exploring the causes and consequences of climatic, geochemical, and evolutionary change in Earth's early history.

6 Code and Data Availability

The current version, which is the exact version of the program used to produce the results used in this paper, as well as the input data and scripts to run the model and produce the plots for all the simulations, is available at https://doi.org/10.5281/zenodo.17966227 (Fernandes (2025)) under the licence GNU General Public License v3.0.

7 Author Contributions

Iris Fernandes and Klaus Mosegaard led the conceptualization of the study and the development of the methodology, including algorithm design, numerical analysis, inverse problem formulation, and the integration of uncertainty quantification. They implemented the data processing and analysis pipeline, contributed to the overall methodological design, and drafted the original manuscript. Tais W. Dahl and Aske Sørensen contributed to the theoretical framework and provided critical input on the geochemical and geological interpretation and analysis. Mohammad Youssof contributed to algorithm parameterization and optimization. Nicholas Thibault contributed with geochronological insights in the analysis.

References

Dahl, T. W., Siggaard-Andersen, M.-L., Schovsbo, N. H., Persson, D. O., Husted, S., Hougård, I. W., Dickson, A. J., Kjær, K., and Nielsen, A. T. (2019). Brief oxygenation events in locally anoxic oceans during the cambrian solves the animal breathing paradox. *Scientific Reports*, 9:11669.

Farhat, M., Auclair-Desrotour, P., Boué, G., and Laskar, J. (2022). The resonant tidal evolution of the earth–moon distance. *Astronomy Astrophysics*, 665:L1.

Fernandes, I. (2025). AstroComb-1.0.

Fernandes, I., Mosegaard, K., and Dahl, T. W. (2026). Probe4t: Geochemically informed sedimentation rate estimation in ultra-high stratigraphic resolution. Submitted to Geoscientific Model Development.

Hays, J. D., Imbrie, J., and Shackleton, N. J. (1976). Variations in the earth's orbit: Pacemaker of the ice ages. *Science*, 194(4270):1121–1132.

Hoang, N., Laskar, J., Hara, N. C., Wu, Y., Sultanov, A., Sinnesael, M., Westerhold, T., and Bujons, P. (2025). Astrogeofit: A genetic algorithm and bayesian approach for the as-

369   tronomical calibration of the geological timescale. *Paleoceanography and Paleoclimatology*,
370   40(8):e2024PA005021.

371   Kemp, D. B. and Sexton, P. F. (2014). Time-scale uncertainty of abrupt events in the
372   geologic record arising from unsteady sedimentation. *Geology*, 42(10):891–894.

373   Laskar, J., Fienga, A., Gastineau, M., and Manche, H. (2011). A new orbital solution for
374   the long-term motion of the earth. *Astronomy Astrophysics*, 532:A89.

375   Laskar, J., Robutel, P., Joutel, F., Gastineau, M., Corrêia, A. C. M., and Levrard, B. (2004).
376   A long-term numerical solution for the insolation quantities of the earth. *Astronomy*
377   *Astrophysics*, 428(1):261–285.

378   Li, M., Kump, L. R., Hinnov, L. A., and Mann, M. E. (2018). Tracking variable sedi-
379   mentation rates and astronomical forcing in phanerozoic paleoclimate proxy series with
380   evolutionary correlation coefficients and hypothesis testing. *Earth and Planetary Science*
381   *Letters*, 501:165–179.

382   Meyers, S. R. (2015). The evaluation of eccentricity-related amplitude modulation and
383   bundling in paleoclimate data: An inverse approach for astrochronologic testing and
384   timescale optimization. *Paleoceanography*, 30(12):1625–1640.

385   Meyers, S. R. (2019). Cyclostratigraphy and the problem of astrochronologic testing. *Earth-*
386   *Science Reviews*, 190:190–223.

387   Meyers, S. R. and Malinverno, A. (2018). Proterozoic milankovitch cycles and the history of
388   the solar system. *Proceedings of the National Academy of Sciences*, 115(25):1717689115.

389   Meyers, S. R., Sageman, B. B., and Hinnov, L. A. (2001). Integrated quantitative stratigra-
390   phy of the cenomanian-turonian bridge creek limestone member using evolutive harmonic
391   analysis and stratigraphic modeling. *Journal of Sedimentary Research*, 71(4):628–644.

392   Meyers, S. R., Sageman, B. B., and Hinnov, L. A. (2008). Resolving milankovitch: Consid-
393   eration of signal and noise. *Paleoceanography*, 23(2):PA2202.

394   Nielsen, A. T., Schovsbo, N. H., Klitten, K., Woollhead, D., and Rasmussen, C. (2018).
395   Gamma-ray log correlation and stratigraphic architecture of the cambro-ordovician alum
396   shale formation on bornholm, denmark: evidence for differential syndepositional isostasy.
397   *Bulletin of the Geological Society of Denmark*, 66:237–273.

398   Sørensen, A. L., Nielsen, A. T., Thibault, N., Zhao, Z., Schovsbo, N. H., and Dahl, T. W.
399   (2020). Astronomically forced climate change in the late cambrian. *Earth and Planetary*
400   *Science Letters*, 548:116475.

401   Waltham, D. (2015). Milankovitch period uncertainties and their impact on cyclostratigra-
402   phy. *Journal of Sedimentary Research*, 85:990–998.

403   Weedon, G. P. (2003). *Time-Series Analysis and Cyclostratigraphy: Examining Stratigraphic*
404   *Records of Environmental Cycles*. Cambridge University Press, Cambridge, UK.

16

Zhao, Z., Thibault, N. R., Dahl, T. W., Schovsbo, N. H., Sørensen, A. L., Rasmussen, C. M. , and Nielsen, A. T. (2022). Synchronizing rock clocks in the late cambrian. *Nature Communications*, 13:1990.